

1

Short Communication

2 **Live Virus Neutralisation of the 501Y.V1 and 501Y.V2 SARS-CoV-2 Variants 3 following INO-4800 Vaccination of Ferrets**

4

5 Shane Riddell¹, Sarah Goldie¹, Alexander J. McAuley¹, Michael J. Kuiper², Peter A. Durr¹, Kim

6 Blasdell¹, Mary Tachedjian¹, Julian D. Druce³, Trevor R.F. Smith⁴, Kate E. Broderick⁴ & Seshadri S.

7 Vasan^{1,5,*}

8

9 ¹Commonwealth Scientific and Industrial Research Organisation, Australian Centre for Disease Preparedness, 5

10 Portarlington Road, East Geelong, VIC 3219, Australia

11 ²Commonwealth Scientific and Industrial Research Organisation, Data61, Docklands, VIC 3008, Australia

12 ³Victorian Infectious Diseases Reference Laboratory, The Royal Melbourne Hospital and The Peter Doherty

13 Institute for Infection and Immunity, 792 Elizabeth Street, Melbourne, VIC 3000, Australia

14 ⁴Inovio Pharmaceuticals, 10480 Wateridge Circle, San Diego, CA 92121, USA

15 ⁵University of York, Department of Health Sciences, York, YO10 5DD, UK

16 *Corresponding Author: vasan.vasan@csiro.au

17

18 **Running Title:** Neutralisation of SARS-CoV-2 Variants following INO-4800 Vaccination

19

20 **Abstract**

21 The ongoing COVID-19 pandemic has resulted in significant global morbidity and mortality on a scale

22 similar to the influenza pandemic of 1918. Over the course of the last few months, a number of

23 SARS-CoV-2 variants have been identified against which vaccine-induced immune responses may be

24 less effective. These “variants-of-concern” have garnered significant attention in the media, with

25 discussion around their impact on the future of the pandemic and the ability of leading COVID-19

26 vaccines to protect against them effectively. To address concerns about emerging SARS-CoV-2

27 variants affecting vaccine-induced immunity, we investigated the neutralisation of representative

28 ‘G614’, ‘501Y.V1’ and ‘501Y.V2’ virus isolates using sera from ferrets that had received prime-boost

29 doses of the DNA vaccine, INO-4800. Neutralisation titres against G614 and 501Y.V1 were
30 comparable, but titres against the 501Y.V2 variant were approximately 4-fold lower, similar to
31 results reported with other nucleic acid vaccines and supported by *in silico* biomolecular modelling.
32 The results confirm that the vaccine-induced neutralising antibodies generated by INO-4800 remain
33 effective against current variants-of-concern, albeit with lower neutralisation titres against 501Y.V2
34 similar to other leading nucleic acid-based vaccines.

35

36 **Introduction**

37 With the continuing roll-out of vaccines against severe acute respiratory syndrome coronavirus 2
38 (SARS-CoV-2), primarily developed against the ancestral 'D614' version of the virus¹, there is concern
39 that emerging 'variants-of-concern' and 'variants-of-interest' may have acquired mutations resulting
40 in lower neutralisation by infection- and vaccine-induced antibodies. Neutralising antibodies are a
41 key correlate of protection against SARS-CoV-2 in humans and non-human primates²⁻⁴, so the
42 determination of antibody-mediated neutralisation against emerging variants is important when
43 assessing vaccine efficacy. Recent publications have demonstrated that these concerns have some
44 basis, with reduced neutralisation of both the '501Y.V1' variant (also called the 'UK variant' or
45 'B.1.1.7') and the '501Y.V2' variant (also called the 'South African variant' or 'B.1.351') by leading
46 mRNA-based vaccines⁵. Similarly, neutralisation studies using human serum samples from
47 coronavirus disease-19 (COVID-19) patients in South Africa reveal significant decreases in
48 neutralisation efficiency against the 501Y.V2 variant^{6,7}.

49

50 We recently investigated the neutralisation of SARS-CoV-2 isolates containing either the 'D614' or
51 the 'G614' variation of the Spike protein, using serum samples from ferrets vaccinated with INO-
52 4800, a leading DNA vaccine candidate against SARS-CoV-2^{8,9}, demonstrating the D614G mutation
53 was unlikely to affect vaccine-induced antibody-mediated virus neutralisation. Given the interest
54 around the 501Y.V1 and 501Y.V2 variants, we decided to follow up our previous study by comparing

55 neutralisation titres of INO-4800-vaccinated ferret samples against representative SARS-CoV-2
56 isolates. We believe such a study is important because: a) DNA vaccines such as INO-4800 can be
57 rapidly modified similar to mRNA vaccines; b) INO-4800 remains stable at room temperature for an
58 extended period, making it especially suitable for combatting the pandemic in resource-poor and
59 remote settings⁹; and, c) INO-4800 has a favourable safety and reactogenicity profile in humans, as
60 demonstrated in clinical trials.

61

62 **Materials and Methods**

63 **Viruses, vaccine, and cells.** Australian SARS-CoV-2 isolates hCoV-19/Australia/VIC31/2020 (VIC31)
64 and hCoV-19/Australia/VIC17990/2020 (VIC17990; 501Y.V1 variant) were provided as Passage 1
65 material by the Victorian Infectious Diseases Reference Laboratory (VIDRL), Melbourne, Australia.
66 hCoV-19/South Africa/KRISP-K005325/2020 (501Y.V2.HV001; 501Y.V2 variant) was provided as
67 Passage 3 material from the Africa Health Research Institute, Durban, South Africa. INO-4800 was
68 provided by Inovio Pharmaceuticals, San Diego, USA, for preclinical testing within the ferret model of
69 COVID-19. This DNA vaccine is a plasmid containing a coding sequence for SARS-CoV-2 (Wuhan-Hu-
70 1) Spike glycoprotein without constraints on protein folding⁹.

71

72 VIC31 Passage 2, VIC17990 Passage 2, and 501Y.V2.HV001 Passage 4 virus stocks were grown in
73 VeroE6 cells (CCL81; American Type Culture Collection (ATCC), Manassas, VA, USA). Briefly, VeroE6
74 cells were grown in 150cm² flasks in Dulbecco's Modified Eagle Medium (DMEM) containing 10%
75 heat-inactivated foetal bovine serum (FBS), 10mM HEPES, 100U/mL penicillin, 100 g/mL
76 streptomycin, and 250ng/mL amphotericin B (all components from ThermoFisher Scientific,
77 Scoresby, VIC, Australia) until 79-90% confluent. The received SARS-CoV-2 isolates were diluted in
78 DMEM containing 10mM HEPES, 100U/mL penicillin, 100 g/mL streptomycin, and 250ng/mL
79 amphotericin B, but no FBS (DMEM-D). Cells were inoculated with 4mL diluted virus and were
80 incubated for 30min at 37°C/5% CO₂ before 40mL DMEM containing 2% FBS, 10mM HEPES,

81 100U/mL penicillin, 100 g/mL streptomycin, and 250ng/mL amphotericin B was added. The flasks
82 were incubated for an additional 48h before supernatant was harvested. ATCC VeroE6 cells were
83 additionally used for virus neutralisation assays (see below).

84

85 **Next-Generation Sequencing.** Virus stocks were sequenced using a MiniSeq platform (Illumina, Inc;
86 San Diego, CA, USA). In brief, 100 μ L cell culture supernatant from the infected Vero E6 cells was
87 combined with 300 μ L TRIzol reagent (Thermo Fisher Scientific) and RNA was purified using a Direct-
88 zol RNA Miniprep kit (Zymo Research; Irvine, CA, USA). Purified RNA was further concentrated using
89 an RNA Clean-and-Concentrator kit (Zymo Research), followed by quantification on a DeNovix DS-11
90 FX Fluorometer. RNA was converted to double-stranded cDNA, ligated then isothermally
91 amplified using a QIAseq FX single cell RNA library kit (Qiagen). Fragmentation and dual-index library
92 preparation was conducted with an Illumina DNA Prep, Tagmentation Library Preparation kit.
93 Average library size was determined using a Bioanalyser (Agilent Technologies; San Diego, CA, USA)
94 and quantified with a Qubit 3.0 Fluorometer (Invitrogen; Carlsbad, CA, USA). Denatured libraries
95 were sequenced on an Illumina MiniSeq using a 300-cycle Mid-Output Reagent kit as per the
96 manufacturer's protocol. Paired-end Fastq reads were trimmed for quality and mapped to the
97 published sequence for the SARS-CoV-2 reference isolate Wuhan-Hu-1 (RefSeq: NC_045512.2) using
98 CLC Genomics Workbench version 21. Variations from the reference sequence were determined
99 with the CLC Genomics Workbench Basic Variant Detection tool set at a minimum frequency of
100 equal to or greater than 35%.

101

102 **Serum samples.** Serum samples used for neutralisation assays were generated and selected with the
103 consent of the sponsor (Coalition for Epidemic Preparedness Innovations), as previously described⁸.
104 In brief, four male and four female ferrets received two doses of INO-4800 via intramuscular
105 administration of 1 mg plasmid DNA to the caudal thigh muscle, followed by electroporation split
106 across two sites using the CELLECTRA[®] device. The prime dose was given on day 0 and the boost on

107 day 28. Sera collected on day 35 or day 42 from three male and three female ferrets were chosen at
108 random to allow for sufficient seroconversion, and to ensure that no ferret provided more than one
109 test sample. Two unvaccinated ferret sera were also included as negative control sera, to ensure
110 that there was no non-specific neutralisation of the viruses. Parent vaccine efficacy studies were
111 approved by the Animal Ethics Committee at CSIRO ACDP (Approval Reference: AEC 2004). No
112 additional ethics approval was required to perform neutralisation assays on serum samples collected
113 from the parent study.

114

115 **Serum dilution.** Each serum sample was diluted 1:20 in DMEM-D (see cell culture methods above) in
116 a deep-well plate on a single occasion, followed by a 2-fold serial dilution in medium across the plate
117 up to 1:20,480. The dilution series for each serum sample was dispensed into triplicate rows of a 96-
118 well plate, for a total volume of 50 μ L per well and triplicate wells per sample dilution.

119

120 **Neutralisation assay.** For the serum-containing wells, 50 μ L virus diluted in medium to contain
121 approximately 100 TCID₅₀ (checked by back-titration) was added to each well. The plates were
122 incubated at 37°C/5% CO₂ for 1h to allow neutralisation complexes to form between the antibodies
123 and the virus. At the end of the incubation, 100 μ L VeroE6 cells (propagated as outlined above for
124 virus stock generation) were added to each well and the plates returned to the incubator for 4 days.
125 Each well was scored for the presence of viral CPE, readily discernible on Day 4 post-infection, with
126 neutralisation titres assigned to each serum replicate based upon the highest dilution that prevented
127 discernible cytopathic effect.

128

129 **Statistical analysis.** Mixed effects analysis of variance (ANOVA) was used to assess differences
130 between SARS-CoV-2 isolates (the fixed effect), with the random effect being the 3 test replicates.
131 For the *post hoc* analysis to detect significant factor level differences we undertook pairwise

132 comparisons with Tukey's adjustment. All analyses were undertaken in R 4.0, using the *nlme* v. 3.1.

133 package for the mixed effects ANOVA modelling and *multcomp* v. 1.4 for the *post hoc* comparisons.

134

135 **Molecular modelling.** Fully glycosylated models of the Spike protein G614, 501Y.V1 and 501Y.V2

136 variants were built based on '6VSB' protein databank (PDB) structure¹⁰ minus transmembrane

137 domains (residues 1161-1272) and included one ACE2 protein bound to the receptor-binding

138 domain. All models were simulated in aqueous solution (TIP3 water, 310K, 0.15M ions, NVT

139 ensemble, each approximately 725,000 atoms in size) using the software NAMD 2.14¹¹ for 150

140 nanoseconds each. Models were visualized with VMD and Nanome^{12,13}.

141

142 **Results**

143 Stocks of VIC31 (hCoV-19/Australia/VIC31/2020; EPI_ISL_419750), the G614 isolate used in our

144 previous study⁸; VIC17990 (hCoV-19/Australia/VIC17990/2020; EPI_ISL_779605), an Australian

145 isolate of the 501Y.V1 variant; and 501Y.V2.HV001 (hCoV-19/South Africa/KRISP-K005325/2020;

146 EPI_ISL_678615), a South African isolate of the 501Y.V2 variant, were propagated and titrated in

147 Vero E6 cells prior to use, with genome sequences confirmed by next-generation sequencing.

148 Mutations within the Spike protein (relative to the reference D614 isolate, Wuhan-Hu-1; RefSeq:

149 NC_045512.2) can be found in **Table 1**.

| Isolate | Mutation | Amino Acid Change | Grantham Distance ^a | Mutation Frequency in Stock |
|-----------------------|-----------------|---------------------|--------------------------------|-----------------------------|
| 501Y.V1 (VIC17990) | A23403G | D614G | 94 | 99.69 |
| | Del21765 (-6nt) | Loss of H69 and V70 | - | 85.83 |
| | Del21991 (-3nt) | Loss of Y144 | - | 94.11 |
| | A23063T | N501Y | 143 | 99.62 |
| | C23271A | A570D | 126 | 99.54 |
| | A23403G | D614G | 94 | 99.82 |
| | C23604A | P681H | 77 | 99.92 |
| | C23709U | T716I | 89 | 99.72 |
| | T24506G | S982A | 99 | 99.76 |
| | G24914C | D1118H | 81 | 100 |
| 501Y.V2 (HV001) | C21614U | L18F | 22 | 100 |
| | A21801C | D80A | 126 | 99.41 |
| | A22206G | D215G | 94 | 99.85 |

| | | | | |
|------------------------------------|-----------------|--------------------------|-----|-------|
| 501Y.V2 (501Y.V2.HV001) | 22281Del (-9nt) | Loss of L242, A243, L244 | - | 75.05 |
| | G22813U | K417N | 94 | 99.71 |
| | G23012A | E484K | 56 | 99.85 |
| | A23063U | N501Y | 143 | 98.65 |
| | A23403G | D614G | 94 | 99.94 |
| | G23593U | Q677H | 24 | 66.36 |
| | C23606U | R682W ^b | 101 | 68.76 |
| | C23664U | A701V | 64 | 99.91 |

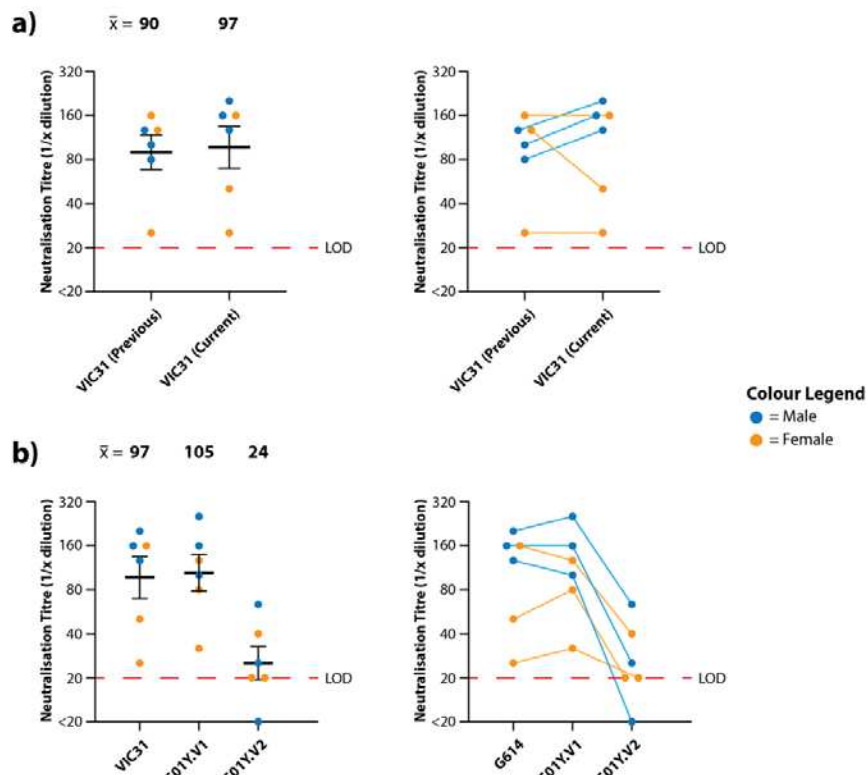
150 **Table 1: Mutations in Spike Protein Present in Variant Stocks (Compared to the Wuhan-Hu-
151 1 Reference Sequence)**

152 ^aGrantham Distance score in the scale of 5 to 215 to quantify the significance of the change
153 based on composition, polarity and molecular volume differences¹⁴; up to 50 is considered
154 'conservative'; 51-100 'moderately conservative'; 101-150 'moderately radical'; 151 and
155 over 'radical'.

156 ^blocated in furin cleavage site

157
158 For consistency and comparison with McAuley et al⁸, microneutralisation assays were performed in
159 triplicate for each serum/isolate combination, using the same three male and three female ferret
160 samples used previously. We additionally included negative control (unvaccinated) ferret serum
161 samples. Neutralisation titres against VIC31 were similar between this study and the previous one⁸
162 (mean neutralisation titre of 90 for previous study; 97 for current study), with no significant
163 difference by mixed effects ANOVA (p>0.05), confirming inter-assay reproducibility (Figure 1a).

164 Mean neutralisation titres were calculated for the different isolates on log₂-transformed data: 97 for
165 VIC31; 105 for 501Y.V1; 24 for 501Y.V2. Mixed effects ANOVA comparison of the neutralisation titres
166 against the three isolates revealed no significant difference in neutralisation of the 501Y.V2 isolate
167 (VIC17990) compared to VIC31, however titres against 501Y.V2 were significantly lower than against
168 the other two (p<0.001; 25% of the VIC31 value; 23% of the 501Y.V1 value) (Figure 1b).



169

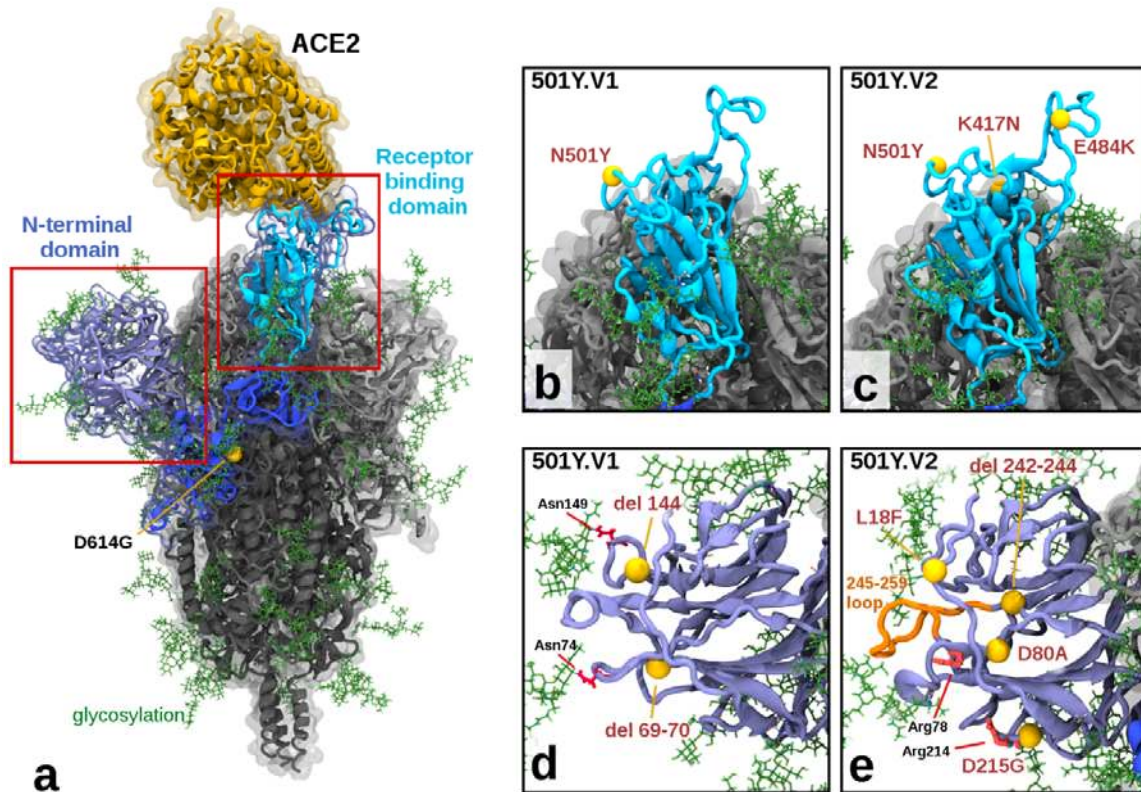
170 **Figure 1: Neutralisation of SARS-CoV-2 Variants-of-Concern with Serum from INO-4800-
171 Vaccinated Ferrets**

172 Neutralisation titres were obtained in triplicate for serum samples collected from ferrets
173 receiving prime and boost doses of INO-4800. a) Comparison of anti-VIC31 (G614 variant)
174 titres from the current and previous studies⁸ demonstrating inter-assay reproducibility (left;
175 $p>0.05$ by paired, two-tailed t-test), and tracking of values from individual animals (right). b)
176 Comparison of neutralisation titres against VIC31 (G614 variant), 501Y.V1 and 501Y.V2
177 variants (left; $p<0.001$ by mixed effects ANOVA), and tracking of values from individual
178 animals (right). Horizontal lines represent geometric mean and geometric standard error of
179 the mean.

180

181 Molecular modelling of the variants shows more cumulative structural changes in 501Y.V2 than
182 501Y.V1 (Figure 2; Table 1), consistent with observed lower neutralisation titres. The receptor-
183 binding domain (RBD) of the Spike protein in the 501Y.V1 variant contains the N501Y mutation,

184 which has been shown to increase binding to the ACE2 receptor^{15,16}, while 501Y.V2 additionally
185 contains the mutations K417N and E484K in the RBD (**Figure 2b,c**). The E484K mutation, although a
186 moderately conservative change in Grantham Distance, has been shown to be an extremely potent
187 escape mutant, showing resistance to many monoclonal and even polyclonal antibodies¹⁷. The
188 K417N mutation, also considered a moderate conservative change, appears to increase hydrogen
189 bonding interactions with the ACE2 receptor via ACE2 N-linked glycosylation at asparagine position
190 Asn90 (**Supplementary Figure S1**). The N-terminal domain (NTD) of the Spike protein in the 501Y.V1
191 variant contains two deletions at residue positions 69-70 and 144, potentially modulating the Spike
192 protein's glycosylation arrangements attached at asparagine residues Asn74 and Asn149. More
193 extensive changes to the NTD exist in the 501Y.V2 variant, with a cluster of mutations (within
194 approximately 15Å radius of D80A), including L18F, the moderately radical D80A, the moderately
195 conservative D215G, and a 242-244 deletion (**Figure 2d,e**). Key implications of these changes within
196 the NTD are: (a) the D80A and D215G mutations in 501Y.V2 have replaced aspartic acid residues
197 which can stabilize salt bridge interactions with the arginine residues Arg78 and Arg214 respectively
198 (**Supplementary Figure S2**); and (b) the 242-244 deletion has removed the 'Leu-Ala-Leu' residues,
199 causing local residue sidechain rearrangement and shortening a solvent exposed loop (residues 245-
200 259), likely altering its antigenic presentation. These combined structural changes in 501Y.V2 could
201 explain our observed reduced inhibition potency relative to the 501Y.V1 and D614G variants.
202



203

204 **Figure 2: Illustration of Mutations in 501Y.V1 and 501Y.V2 Relative to the Ancestral Form**

205 a) Structure of the glycosylated SARS CoV2 Spike protein highlighting a S1 monomer (in
206 blues) and relative positions of the N terminal domain (NTD) and the receptor-binding
207 domain (RBD) and the bound ACE2 receptor (in yellow). The position of D614G (common to
208 all tested variants) is also highlighted. b) & c) Side by side comparison of 501Y.V1 and
209 501Y.V2 variants in the RBD, showing the V2 variant having additional K417N and E484K
210 mutations. d) & e) Side by side comparisons of 501Y.V1 and 501Y.V2 variants in the NTD,
211 showing relative locations of mutations and deletions. (Model files available in
212 Supplementary Materials).

213

214 **Discussion**

215 The results of this study are consistent with previous analyses of the effect of emerging SARS-CoV-2
216 variants on infection- and vaccine-induced immune responses⁵⁻⁷. Indeed, the reductions in

217 neutralisation titres (and by extension, vaccine-induced protection) observed with the 501Y.V2
218 variant are comparable for leading nucleic acid based COVID-19 vaccines – approximately 4-fold for
219 INO-4800 (Inovio Pharmaceuticals), compared to 6.5-fold for BNT162b2 (BioNTech/Pfizer) and 8.6-
220 fold for mRNA-1273 (Moderna) – and substantially less than the 86-fold reduction reported for
221 AZD1222 (Oxford/AstraZeneca)⁵. We observed no decrease in neutralisation titre with 501Y.V1
222 versus G614, compared to other leading vaccines, however host-specific effects may play a role⁵. It is
223 encouraging that INO-4800-vaccinated ferret serum maintains neutralisation efficacy against the
224 spectrum of emerging ‘variants-of-concern’ evaluated by this study¹⁸; this is consistent with the
225 maintenance of neutralisation of pseudovirus prototypes of SARS-CoV-2 variants with serum
226 samples from human recipients of the INO-4800 vaccine¹⁹. Our study indicates that nucleic acid-
227 based vaccines will have an important role to play in this pandemic, in terms of their general ability
228 to maintain neutralisation efficacy and to be modified for ‘vaccine matching’ in the future.

229

230 **References**

- 231 1 Korber, B. *et al.* Tracking Changes in SARS-CoV-2 Spike: Evidence that D614G Increases
232 Infectivity of the COVID-19 Virus. *Cell* **182**, 812-827.e819,
233 doi:<https://doi.org/10.1016/j.cell.2020.06.043> (2020).
- 234 2 Lau, E. H. Y. *et al.* Neutralizing antibody titres in SARS-CoV-2 infections. *Nature
235 Communications* **12**, 63, doi:10.1038/s41467-020-20247-4 (2021).
- 236 3 McMahan, K. *et al.* Correlates of protection against SARS-CoV-2 in rhesus macaques. *Nature*
237 **590**, 630-634, doi:10.1038/s41586-020-03041-6 (2021).
- 238 4 Brown, M. Immune correlates of SARS-CoV-2 protection. *Nature Reviews Immunology* **20**,
239 593-593, doi:10.1038/s41577-020-00442-6 (2020).
- 240 5 Abdool Karim, S. S. & de Oliveira, T. New SARS-CoV-2 Variants - Clinical, Public Health, and
241 Vaccine Implications. *N Engl J Med*, doi:10.1056/NEJMc2100362 (2021).

242 6 Wibmer, C. K. *et al.* SARS-CoV-2 501Y.V2 escapes neutralization by South African COVID-19
243 donor plasma. *Nat Med*, doi:10.1038/s41591-021-01285-x (2021).

244 7 Cele, S. *et al.* Escape of SARS-CoV-2 501Y.V2 from neutralization by convalescent plasma.
245 *Nature*, doi:10.1038/s41586-021-03471-w (2021).

246 8 McAuley, A. J. *et al.* Experimental and in silico evidence suggests vaccines are unlikely to be
247 affected by D614G mutation in SARS-CoV-2 spike protein. *npj Vaccines* **5**, 96,
248 doi:10.1038/s41541-020-00246-8 (2020).

249 9 Smith, T. R. F. *et al.* Immunogenicity of a DNA vaccine candidate for COVID-19. *Nature*
250 *Communications* **11**, 2601, doi:10.1038/s41467-020-16505-0 (2020).

251 10 Wrapp, D. *et al.* Cryo-EM structure of the 2019-nCoV spike in the prefusion conformation.
252 *Science* **367**, 1260, doi:10.1126/science.abb2507 (2020).

253 11 Phillips, J. C. *et al.* Scalable molecular dynamics with NAMD. *J Comput Chem* **26**, 1781-1802,
254 doi:10.1002/jcc.20289 (2005).

255 12 Humphrey, W., Dalke, A. & Schulten, K. VMD: Visual molecular dynamics. *Journal of*
256 *Molecular Graphics* **14**, 33-38, doi:[https://doi.org/10.1016/0263-7855\(96\)00018-5](https://doi.org/10.1016/0263-7855(96)00018-5) (1996).

257 13 Nanome: Creating Powerful, Collaborative and Scientific VR Tools (San Diego, CA, 2020).

258 14 Grantham, R. Amino Acid Difference Formula to Help Explain Protein Evolution. *Science* **185**,
259 862, doi:10.1126/science.185.4154.862 (1974).

260 15 Starr, T. N. *et al.* Deep Mutational Scanning of SARS-CoV-2 Receptor Binding Domain Reveals
261 Constraints on Folding and ACE2 Binding. *Cell* **182**, 1295-1310.e1220,
262 doi:<https://doi.org/10.1016/j.cell.2020.08.012> (2020).

263 16 Tian, F. *et al.* Mutation N501Y in RBD of Spike Protein Strengthens the Interaction between
264 COVID-19 and its Receptor ACE2. *bioRxiv*, 2021.2002.2014.431117,
265 doi:10.1101/2021.02.14.431117 (2021).

266 17 Greaney, A. J. *et al.* Comprehensive mapping of mutations in the SARS-CoV-2 receptor-
267 binding domain that affect recognition by polyclonal human plasma antibodies. *Cell Host*
268 *Microbe* **29**, 463-476, doi:10.1101/2020.12.31.425021 (2021).
269 18 Garcia-Beltran, W. F. *et al.* Multiple SARS-CoV-2 variants escape neutralization by vaccine-
270 induced humoral immunity. *Cell*, doi:10.1016/j.cell.2021.03.013 (2021).
271 19 Andrade, V. M. *et al.* INO-4800 DNA vaccine induces neutralizing antibodies and T cell
272 Activity against global SARS-CoV-2 variants. *bioRxiv*,
273 doi:<https://doi.org/10.1101/2021.04.14.439719> (2021).
274

275 **Data Availability Statement**

276 The data that support the findings of this study are available through the corresponding author upon
277 reasonable request. Next generation sequencing data for the virus stocks is available from the NCBI
278 BioProject database (BioProject ID: PRJNA722318).
279

280 **Acknowledgements**

281 We are grateful for support from our colleagues at the Australian Centre for Disease Preparedness
282 (<https://www.grid.ac/institutes/grid.413322.5>), particularly those in the Dangerous Pathogens and
283 Animal Studies Teams who performed the parental vaccine study, and Kristen McAuley who
284 facilitated importation of SARS-CoV-2 variants. The authors would like to thank the Victorian
285 Infectious Diseases Reference Laboratory (especially Dr Mike Catton) for providing the VIC31 and
286 VIC17990 (501Y.V1) isolates, and Tulio de Oliveira and Alex Sigal for providing the 501Y.V2.HV001
287 isolate. This work was conducted with funding to the Commonwealth Scientific and Industrial
288 Research Organisation from the Australian Department of Finance, the Coalition for Epidemic
289 Preparedness Innovations, and Inovio Pharmaceuticals, Inc.
290

291 **Competing Interests**

292 T.R.F.S. and K.E.B. are the co-inventors of INO-4800 and employees of Inovio Pharmaceuticals, but
293 did not play a role in data acquisition or analysis. T.R.F.S. and K.E.B. receive salary and benefits,
294 including ownership of stock and stock options, from the company. Other authors declare no
295 competing interests.

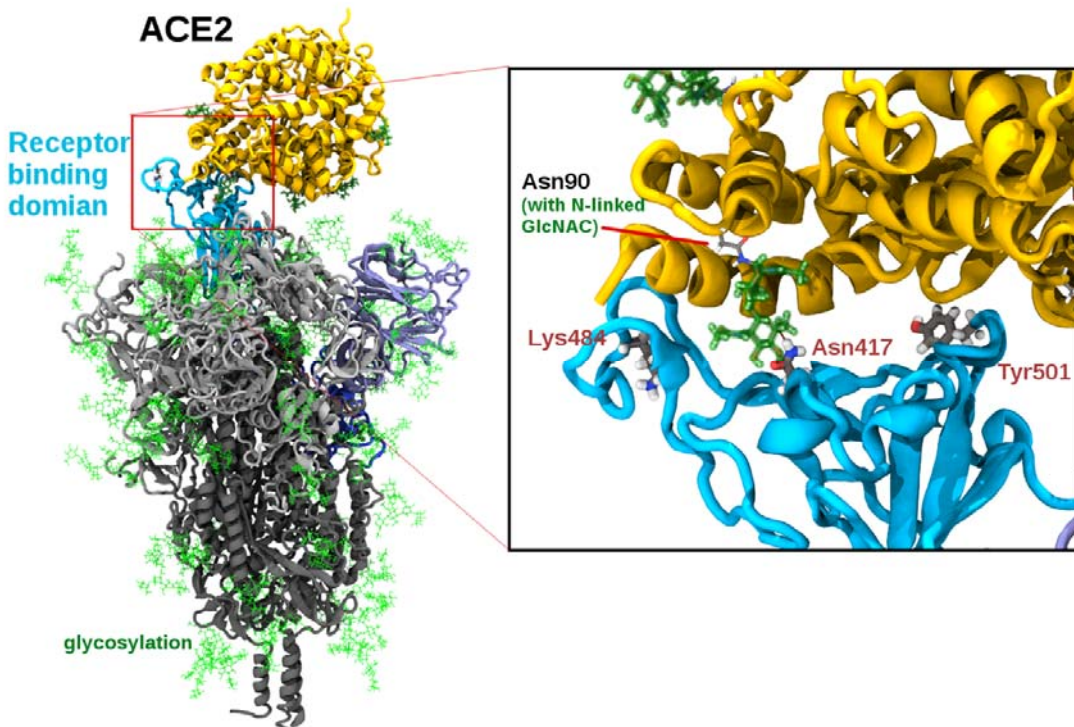
296

297 **Author Contributions**

298 A.J.M., P.A.D., and S.S.V. designed the study. S.R., S.G., A.J.M., and K.B. performed the experiments.
299 A.J.M., P.A.D., and M.T. analysed the experimental data. M.J.K. performed biomolecular modelling
300 and provided structural interpretations. J.D.D. isolated VIC31 and VIC17990 virus isolates; T.R.F.S.
301 and K.E.B. co-invented the vaccine used in this study. A.J.M., P.A.D., M.J.K. and S.S.V. co-wrote the
302 manuscript and made revisions. S.S.V. conceived the project and obtained funding. All authors
303 reviewed the manuscript.

304

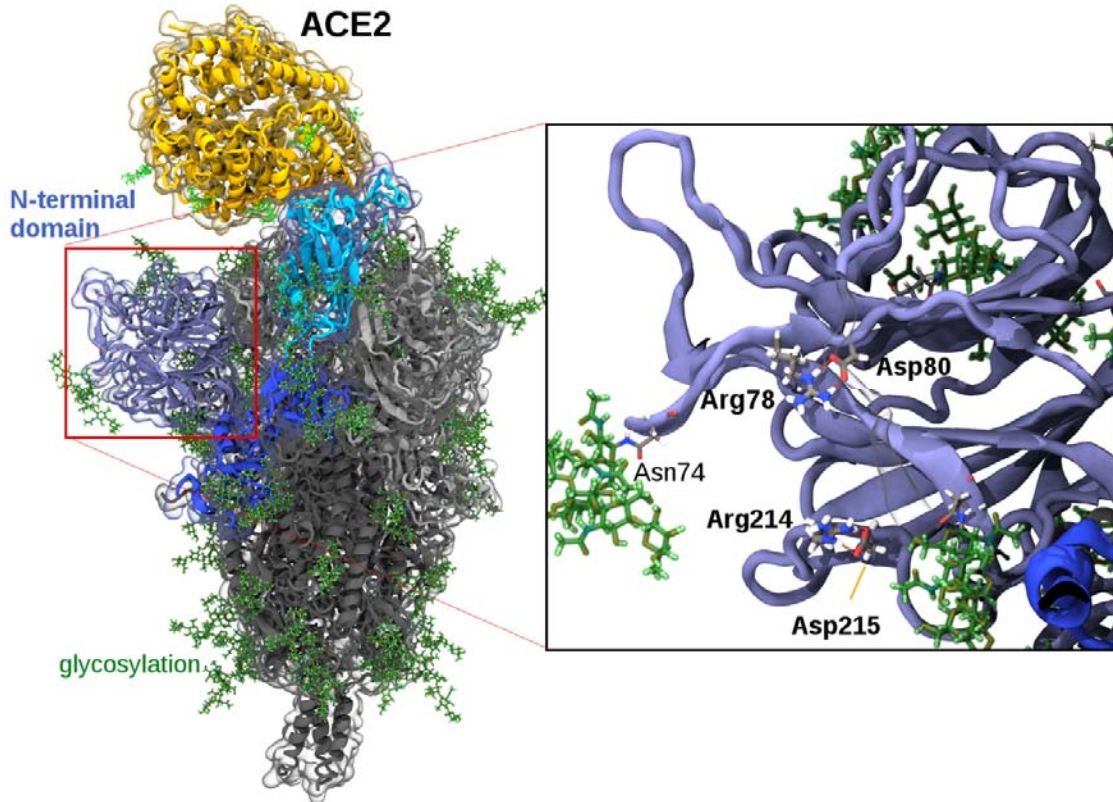
305 **Supplementary Figures**



306

307 **Supplementary Figure 1.** Structure of ACE2 binding to the SARS-CoV-2 Spike receptor-binding
308 domain of variant 501Y.V2. Modelling suggests the lysine to asparagine mutation, (K417N), may
309 facilitate additional hydrogen bonding to the ACE2 receptor, (Angiotensin-converting enzyme 2), via
310 binding through an N-linked glycoside at position asparagine Asn90 in ACE2. (In this case modelled
311 as Beta-D-GlcNAc (1->4) GlcNAc). The relative position of the other 501Y.V2 mutations in the
312 receptor-binding domain (Tyr501 and Lys484) as also shown.

313



314

315 **Supplementary Figure 2.** Structure of ACE2 binding to the SARS-CoV-2 Spike receptor-binding
316 domain showing a close up of the N-terminal domain region, highlighting the salt bridges between
317 arginine and aspartic acid at positions Arg78-Asp80 and Arg214-Asp215. In the 501Y.V2 variant,
318 aspartic acid 80 is mutated to alanine (D80A) and aspartic acid 215 is mutated to glycine (D215G),
319 losing both salt bridges, altering the relative positions of the arginine residues, as shown in Figure
320 2e). The asparagine N-linked glycosylation attachment point Asn74 is also labelled in the diagram.